Exhibit F

LETTERS

A paracrine requirement for hedgehog signalling in cancer

Robert L. Yauch[1]*, Stephen E. Gould[1]*, Suzie J. Scales[1], Tracy Tang[1], Hua Tian[1], Christina P. Ahn[1], Derek Marshall[1], Ling Fu[1], Thomas Januario[1], Dara Kallop[1], Michelle Nannini-Pepe[1], Karen Kotkow[2]†, James C. Marsters Jr[1], Lee L. Rubin[2]† & Frederic J. de Sauvage[1]

Ligand-dependent activation of the hedgehog (Hh) signalling pathway has been associated with tumorigenesis in a number of human tissues[1–7]. Here we show that, although previous reports have described a cell-autonomous role for Hh signalling in these tumours[1–7], Hh ligands fail to activate signalling in tumour epithelial cells. In contrast, our data support ligand-dependent activation of the Hh pathway in the stromal microenvironment. Specific inhibition of Hh signalling using small molecule inhibitors, a neutralizing anti-Hh antibody or genetic deletion of smoothened (*Smo*) in the mouse stroma results in growth inhibition in xenograft tumour models. Taken together, these studies demonstrate a paracrine requirement for Hh ligand signalling in the tumorigenesis of Hh-expressing cancers and have important implications for the development of Hh pathway antagonists in cancer.

An increasing number of solid tumours have been reported to be reliant on ligand-dependent Hh pathway signalling within the tumour epithelium[1–7]. Because the typical role for Hh in development is mediated by paracrine effects on mesenchymal cells[8,9], we wanted to explore further the mechanisms behind Hh-dependent tumorigenesis. We have evaluated the effect of a specific and potent small molecule SMO-acting antagonist of the Hh pathway (HhAntag) on cell viability across a large panel of cancer cell lines (Fig. 1a)[10,11]. HhAntag has been demonstrated to be ~10-times more potent than the natural product SMO antagonist, cyclopamine, at inhibiting Hh pathway activity[10]. We observed a range of cellular sensitivities to HhAntag with half-maximal inhibitory concentration (IC_{50}) values for growth inhibition ranging from ~2 μM to >30 μM. In contrast to previous reports[6,7], no tissue specificity of *in vitro* sensitivity to HhAntag was observed. The extent of basal Hh pathway activity in these cell lines, as measured by the expression of *GLI1*, a well characterized endogenous direct transcriptional target gene, did not correlate with cellular sensitivity to HhAntag (Fig. 1a), nor could we detect a positive correlation between cellular sensitivity and other Hh pathway genes (Supplementary Fig. 1 and Supplementary Table 1). Finally, these differences were not a unique attribute of the synthetic small molecule HhAntag, as a similar discordance of all variables was observed with cyclopamine (Supplementary Fig. 2)[12].

The requirement for high concentrations of HhAntag or cyclopamine to elicit growth inhibition and the lack of correlation with Hh pathway activation suggested that the observed *in vitro* growth repression might be due to non-specific effects of these molecules. This is supported by the observation that only 100 nM HhAntag is needed to completely inhibit Hh signalling in a Hh-responsive human mesenchymal cell line (HEPM) expressing a *GLI* luciferase reporter construct (HEPM-rep, Fig. 1b) and the IC_{50} of 5 nM is ~400-times lower than that required to inhibit cell growth by 50% in the most sensitive cancer cell line (1.9 μM). To address specifically whether the *in vitro* growth inhibitory effect of high concentrations of Hh antagonists is due to off-target activity, we focused on two pancreatic cell lines described recently: CFPAC-1, a SMO-positive and cyclopamine-sensitive cell line, and BxPC-3, a SMO-negative cell line with differentially reported sensitivity to cyclopamine[4,6,13]. Despite differences in *SMO* expression (Supplementary Table 1), we found that these cell lines exhibit similar sensitivities to the growth inhibitory effects of high concentrations of cyclopamine and HhAntag (Fig. 1a, b). Conversely, no growth inhibition was observed using two completely different mechanisms of Hh pathway inhibition: PKA activation using the agonist forskolin[14] (Fig. 1c) or the anti-Hh ligand blocking antibody 5E1 (Fig. 1d). Finally, neither Hh pathway activation with recombinant Sonic hedgehog homologue (rSHH) nor pathway inhibition with high concentrations (10 μM) of Hh antagonists had any effect on endogenous *GLI1* messenger RNA levels in these cells (Fig. 1e), despite regulating pathway activity in HEPM cells. Previous reports relied on transfected *GLI* reporter constructs to monitor endogenous Hh pathway activity. rSHH was unable to activate *GLI* reporter activity when transfected into either CFPAC-1 or BxPC-3 cells (Supplementary Fig. 3). Although high concentrations of HhAntag and cyclopamine inhibited *GLI* reporter activity in CFPAC-1 and BxPC-3 cells, comparable repressions of unrelated transcriptional reporters were also observed at these high concentrations (Supplementary Fig. 4). Similar effects of Hh antagonists on viability and signalling were observed across a variety of cell lines that have been used previously (Supplementary Fig. 5)[5–7]. Taken together, the data strongly argue against Hh signalling in these epithelial cancer cell lines and suggest that the previously observed effects of Hh antagonists on growth and reporter activity are due to off-target effects of these molecules when used at high concentrations.

Despite our failure to detect Hh pathway activity in epithelial cells *in vitro*, we determined that subsets of human tumours and cell lines do indeed express Hh ligands. Microarray expression analysis of human tissue specimens revealed that subsets of colorectal, endometrial, ovarian and pancreatic cancers overexpressed Hh ligand mRNA (data not shown). Quantitative polymerase chain reaction with reverse transcription (RT–PCR) profiling of an independent set of human tissue specimens confirmed that the transcript levels of *SHH* and/or Indian hedgehog homologue (*IHH*) ligands were significantly upregulated in subsets of these cancers (Fig. 2a–c). In contrast, we did not observe increased *SHH* or *IHH* expression in a smaller panel of lung cancer specimens (Fig. 2d). Differential expression of SHH and

[1]Genentech Inc., 1 DNA Way, South San Francisco, California 94080, USA. [2]Curis Inc., 45 Moulton Street, Cambridge, Massachusetts 02138, USA. †Present address: Harvard Stem Cell Institute, Harvard University, Biolabs Room 1065, 16 Divinity Avenue, Cambridge, Massachusetts 02138, USA.
*These authors contributed equally to this work.

IHH mRNA and protein was recapitulated in cancer cell lines representative of these tissue types (Supplementary Figs 6 and 7). To determine whether the ligands produced by these cancer cell lines are functional, we co-cultured these cells with 10T1/2 cells stably transfected with a *GLI* reporter construct (Fig. 2e). The induction of *GLI* reporter activity in the fibroblasts correlated with the levels of ligand produced by the tumour cells, demonstrating their capacity to stimulate paracrine signalling. To establish whether a similar paracrine-mediated activation could occur *in vivo*, xenografts were established in *Ptch1-lacZ;Rag2*$^{-/-}$ mice from the pancreatic cell lines HPAF-II and PL45, which differ in expression of Hh ligands (Supplementary Fig. 6). Anti-β-galactosidase staining of Hh-positive HPAF-II xenografts resulted in labelling of stromal cells immediately adjacent to the tumour cell compartment (Fig. 2f and Supplementary Fig. 8). In contrast, β-galactosidase staining was not observed in the stroma of xenografts derived from PL45 cells, which express very low levels of Hh ligands. Taken together, these results demonstrate that Hh-expressing tumour epithelial cells are capable of activating the Hh pathway in a paracrine manner, both *in vitro* and *in vivo*.

To uncover the role of paracrine Hh signalling in regulation of tumour growth and to ensure that the lack of Hh signalling in cell lines was not a feature of cell culture[15], we first used models in which tumour cells had never been grown *in vitro*. We generated mouse xenograft models from surgical biopsies of patients harbouring a variety of neoplasms. On implantation of these primary tumours

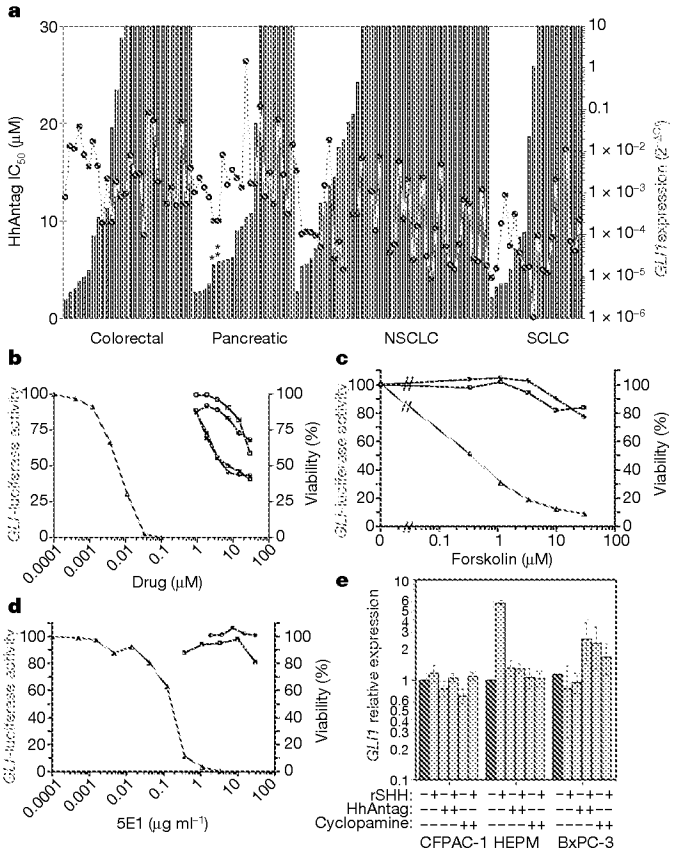

Figure 1 | Lack of Hh pathway activation in human cancer cell lines. **a**, No association was shown between Hh antagonist-mediated growth inhibition (IC_{50}, left *y* axis, solid bars) and quantitatively determined Hh target gene expression (*GLI1*, right *y* axis, blue dots). BxPC-3 and CFPAC-1 cells are highlighted by single and double asterisks, respectively. NSCLC, non-small-cell lung cancer; SCLC, small-cell lung cancer. **b**–**d**, Equivalent degrees of growth inhibition mediated by Hh pathway antagonists in a *SMO*-positive (CFPAC-1, squares) compared to a *SMO*-negative (BxPC-3, circles) cell line. The concentration of antagonists required to inhibit Hh pathway activity was determined by measuring luciferase activity (red line) in a cell line expressing a Hh-responsive *GLI*-luciferase reporter (HEPM-rep, triangles). Hh pathway antagonists include cyclopamine (**b**, open symbols), HhAntag (**b**, filled symbols), forskolin (**c**) and the anti-Hh-ligand-blocking antibody 5E1 (**d**). **e**, Both SHH (rSHH, 1 μg ml^{-1}) and Hh antagonists (10 μM) fail to modulate endogenous Hh target genes in cancer cells. Human embryonic palatal mesenchyme (HEPM) serves as a positive control. Error bars, mean ± s.d. ($n = 3$).

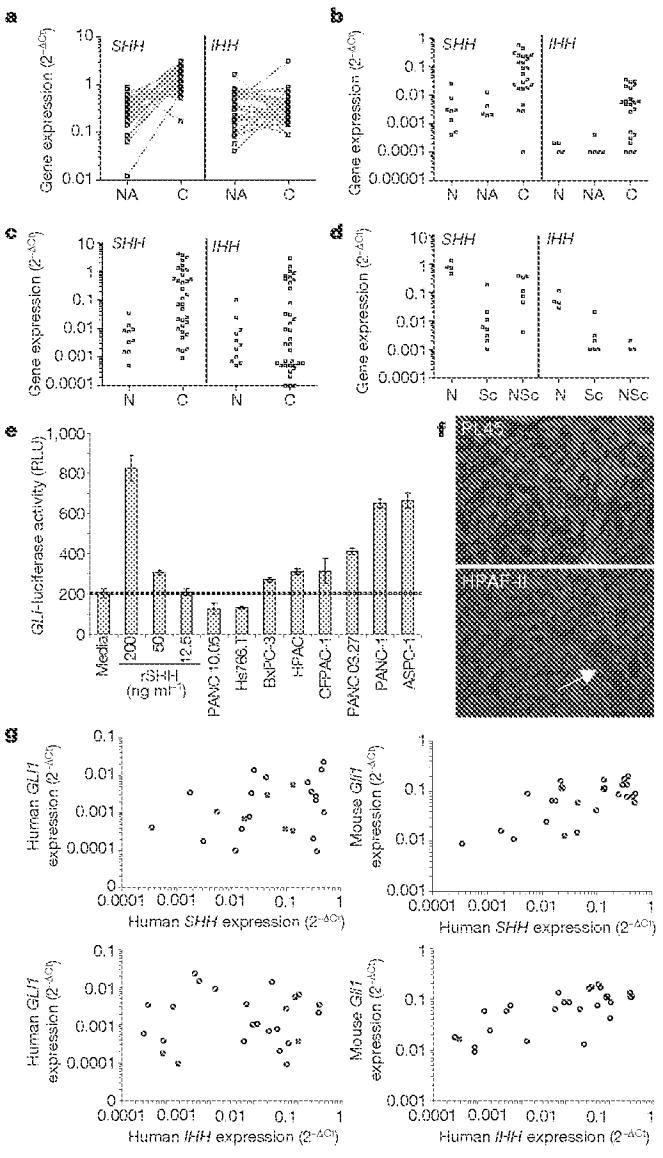

Figure 2 | Human Hh ligands are overexpressed in a subset of human cancers and can activate Hh signalling in a paracrine manner. Quantitative RT–PCR profiling of *SHH* and *IHH* mRNA in a subset of human tissues: **a**, colorectal; **b**, pancreatic; **c**, ovarian; and **d**, lung, SCLC (Sc) and NSCLC (NSc). Colorectal tissue is patient-matched. C, primary tumour tissue; N, normal; NA, normal adjacent. **e**, Induction of Hh-responsive reporter activity in 10T1/2-rep fibroblasts after co-culture with pancreatic cells or rSHH. Error bars, mean ± s.d. ($n = 3$). RLU, relative luciferase units. **f**, Stromal activation of the Hh pathway activity in HPAF-II, but not PL45, xenografts *in vivo*. β-galactosidase activity (red) was observed in the stromal compartment after implantation of HPAF-II cells in *Ptch1-lacZ;Rag2*$^{-/-}$ mice; epithelial-specific antigen is shown in green. Arrow shows β-galactosidase-positive cells. **g**, Correlation between stromal-derived, but not tumour-derived, *Gli1* mRNA levels versus tumour-derived Hh ligand (*SHH* and *IHH*) levels in primary human tumour xenografts ($n = 22$, $P = 0.005$ *SHH/Gli1*; $P = 0.0003$ *IHH/Gli1*) by species-specific qRT–PCR. The red and blue dots refer to the xenograft models in Fig. 3a (blue, D5123; red 1051178-A).

in nude mice, human-derived stroma is rapidly replaced by host mouse stroma (Supplementary Fig. 9)[16]. To differentiate Hh pathway activity in the tumour versus stromal compartments, species-specific primer/probe sets were generated to detect human tumour versus mouse stromal pathway genes (Supplementary Table 2). We observed a statistically significant correlation between the levels of *SHH* and *IHH* expression in the tumour and activation of Hh signalling, as judged by *Gli1* (Fig. 2g, right panels) and *Ptch1* (data not shown), in the stroma. This correlation was not detected within the tumour compartment alone (Fig. 2g, left panels, *GLI1*). Human *PTCH1* mRNA was also evaluated by qRT–PCR and no correlation was observed with human *SHH* or *IHH* in the tumour compartment (data not shown). Overall, the absolute level of *Gli1* expression in the stromal infiltrate of individual xenografts was higher compared to those originating from the tumour epithelium (Supplementary Fig. 10). Taken together, these data support a model in which Hh ligands produced by the tumour cells activate the pathway in the surrounding stroma.

To address whether tumours producing Hh ligands are dependent on the paracrine activation of the Hh pathway for growth, xenografts were generated from biopsies of patients with pancreatic adenocarcinoma (1051178-A) and colon adenocarcinoma (D5123). Both models express significant levels of *SHH* and/or *IHH* mRNA (Fig. 2g). D5123 tumours did not express any detectable *SMO* mRNA in the tumour epithelium (cycling threshold, $C_t = 39$). Oral administration of HhAntag to mice harbouring these primary human xenografts resulted in significant growth delay in both models (Fig. 3a), with average tumour growth inhibitions of 29% and 48%, respectively. Significantly, the doses of HhAntag required to inhibit growth were similar to the doses required to fully inhibit endogenous Hh target genes in tumour stroma or in surrogate normal tissues, suggesting that growth inhibition is a specific consequence of Hh inhibition (Supplementary Fig. 11). Next we analysed a panel of colon cell lines with differential levels of Hh ligand expression. Whereas HT55 and HT-29 cells expressed increased levels of both SHH and IHH, neither ligand was detectable in DLD-1 cells (Supplementary Figs 6 and 7). Furthermore, HT-29 cells did not express detectable *SMO* mRNA ($C_t = 40$). HhAntag treatment resulted in a statistically significant growth delay of HT55 and HT-29 xenografts compared to vehicle controls, whereas HhAntag had no effect on the growth of DLD-1 xenografts (Fig. 3b). Furthermore, the *in vivo* activity was not reflective of the activity observed *in vitro* (Fig. 1a and Supplementary Fig. 5). To demonstrate further that the growth delay observed with HhAntag is specific, mice harbouring HT55 and HT-29 xenografts were treated with the Hh ligand-blocking antibody 5E1. Analogous to the degree of growth inhibition observed with HhAntag, 5E1 resulted in a statistically significant growth retardation in both models (Fig. 3c). In all xenografts tested, Hh pathway antagonist treatment resulted in the downregulation of canonical Hh target genes in the stromal microenvironment, but not within the tumour epithelium, as determined by species-specific expression profiling (Fig. 4a, b and data not shown). Overall, these data suggest that the growth effect mediated by Hh pathway inhibition is by means of its action on the stromal microenvironment and is consistent with a paracrine signalling mechanism.

Finally, to validate further the contribution of Hh-activated stroma to tumour growth, we assessed the ability of fibroblasts deficient in Hh signalling to support the growth of HT-29 cells expressing luciferase (HT29-*luc*). Mouse embryonic fibroblasts (MEFs) were isolated from mice engineered to conditionally remove *Smo* on tamoxifen induction of Cre recombinase activity (*CAGGCreER;* $Smo^{C/C}$) [17,18]. After tamoxifen treatment, induction of Cre activity led to a greater than 85% reduction in *Smo* expression (Supplementary Fig. 12), and near complete inhibition of *Gli1* upregulation in response to Hh stimulation when compared to control ($Smo^{C/C}$) MEFs (Fig. 4c). Whereas implantation of a suboptimal number of HT29-*luc* cells in mice did not result in measurable tumours at 26 days post-implantation, co-injection of HT29-*luc* cells with tamoxifen-treated MEFs from *CAGGCreER;*$Smo^{C/C}$ mice resulted in smaller tumours compared to HT29-*luc* cells co-injected with $Smo^{C/C}$ control MEFs (Fig. 4d). Imaging of mice revealed a significant decrease in luciferase activity in mice implanted with HT29-*luc*/*CAGGCreER;*$Smo^{C/C}$ MEFs compared to HT29-*luc*/$Smo^{C/C}$ MEFs, demonstrating that the tumour size differences were indeed caused by differences in HT29-*luc* growth (Fig. 4e, f). These data demonstrate that Hh activity in the stromal microenvironment can provide a growth advantage to tumour cells.

We have found that tumours overexpressing Hh ligand(s) activate the signalling pathway in neighbouring stromal cells. This conclusion differs from that presented in several recent publications, the conclusions of which were largely based on inhibition of proliferation using high concentrations of Hh pathway antagonists, as well as the use of artificial reporter constructs to monitor Hh pathway activity. Although we cannot rule out a potential role for Hh signalling in a

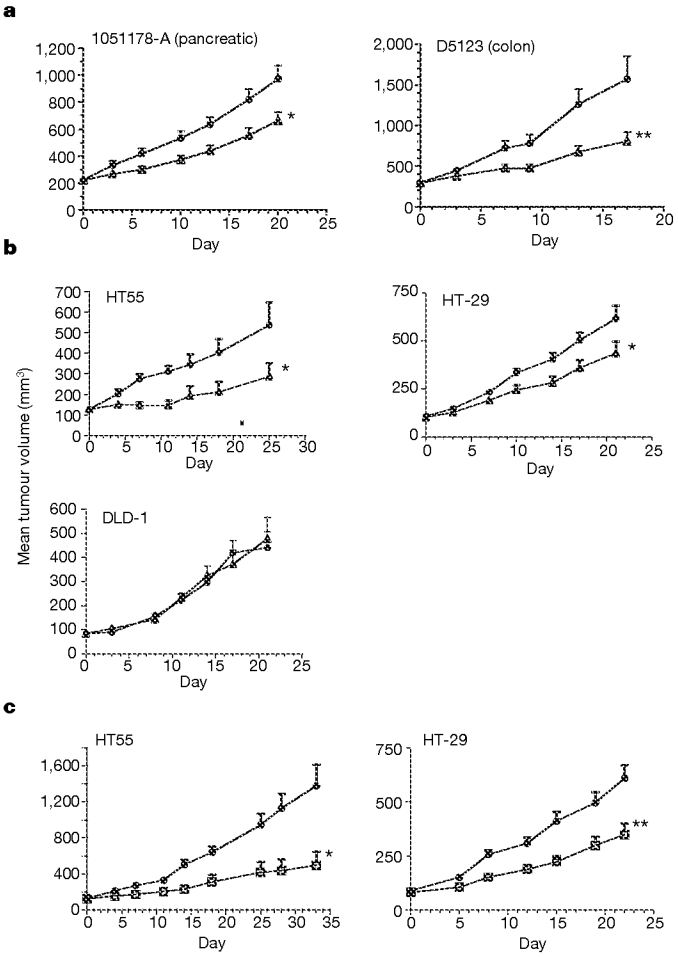

Figure 3 | Inhibition of the Hh pathway results in a significant delay in the growth of Hh ligand-expressing tumours *in vivo*. **a**, Change in tumour volume in two primary human tumour xenograft models after treatment with vehicle (filled circles) or Hh antagonists (open triangles; 75 mg kg^{-1} twice daily for 1051178-A and 100 mg kg^{-1} twice daily for D5123); $^{*}P < 0.001$, $^{**}P < 0.05$ ($n = 11$ per arm, 1051178-A; $n = 8$ per arm, D5123). **b**, Change in tumour volume in three colorectal cell line xenografts after treatment with vehicle (filled circles) or HhAntag (open triangles; 75 mg kg^{-1} twice daily for HT-29, 100 mg kg^{-1} twice daily for HT55 and DLD-1); $^{*}P < 0.05$ ($n = 11$ per arm, HT55; $n = 10$ per arm, DLD-1; $n = 20$ vehicle arm, $n = 15$ HhAntag arm, HT-29). **c**, Change in tumour volume in two Hh-positive colorectal cell line xenografts after treatment with an isotype control IgG (filled circles) or 5E1 (open squares); $^{*}P < 0.01$; $^{**}P < 0.05$ ($n = 10$ per arm, both models). Data in all panels are expressed as mean tumour volumes ± s.e.m.

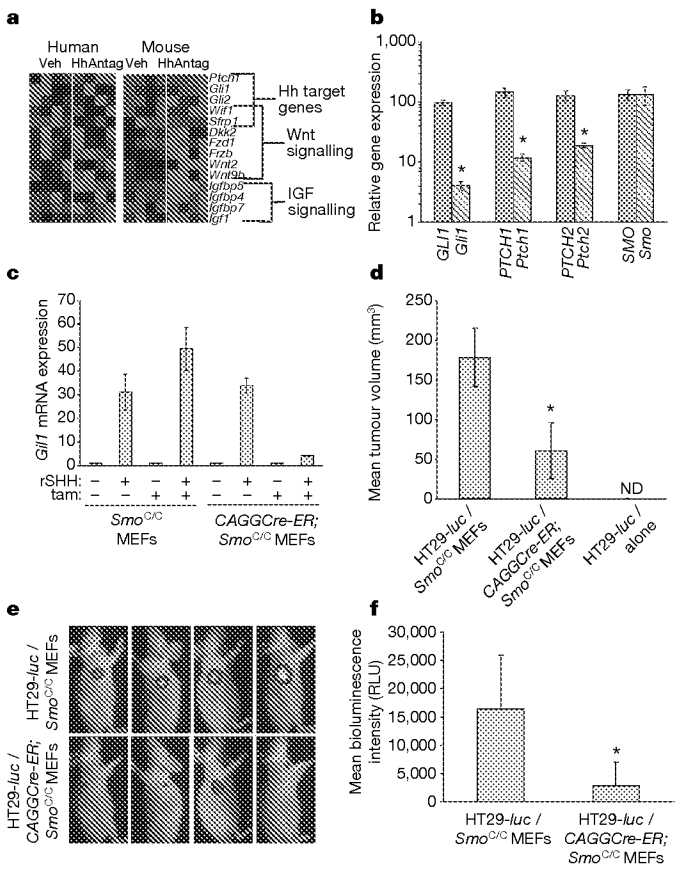

Figure 4 | Stromal hedgehog signalling can support tumour growth. a, Heat map representing mRNA expression of selected human and mouse genes in p1051178-A xenografts after treatment with vehicle (Veh) or Hh antagonist (HhAntag). Red, high expression; green, low expression. IGF, insulin-like growth factor. **b**, Hh antagonist treatment results in repression of stromal-derived (hatched bars, $*P < 0.01$), but not tumour-derived (solid bars), Hh target genes in 1051178-A xenografts ($n = 5$), as assessed by species-specific qRT–PCR. **c**, Inability of rSHH stimulation to induce *Gli1* mRNA in tamoxifen-treated MEFs derived from *CAGGCreER;Smo*$^{C/C}$ mice compared to *Smo*$^{C/C}$ MEFs ($n = 3$). **d**, Reduction in tumour size 26 days after the implantation of 3×10^5 HT29-*luc* cells with 1.5×10^6 of tamoxifen-treated *CAGGCreER;Smo*$^{C/C}$ MEFs compared to *Smo*$^{C/C}$ MEFs. ND, not detected ($n = 4$). **e**, *In vivo* imaging of HT29-*luc* tumour cells in **d**. **f**, Quantified bioluminescent images of HT29-*luc* tumour cells in **e** ($*P = 0.04$). All data are expressed as means ± s.d.

minor subpopulation of epithelial tumour cells such as self-renewing cancer stem cells[19], an epithelia-to-mesenchyma signalling paradigm has been well described for Hh in various non-neoplastic settings[9] and data are beginning to emerge that support this paradigm in neoplastic models[20]. How Hh pathway inhibition in the stromal microenvironment suppresses tumour growth remains to be elucidated. Hh-driven mesenchymal signals could influence the structural interactions between the tumour epithelium and its microenvironment or stromal Hh signalling could affect the expression of soluble factors in the tumour microenvironment that are used by either the tumour epithelium or additional stromal cell types. Stimulation of the Hh pathway in mesenchymal cells has been shown to regulate genes and pathways that are involved in tumorigenesis and metastasis[21,22]. We find that inhibition of Hh signalling in the stroma can modulate factors, such as insulin-like growth factor receptor and Wnt signalling pathway components (Fig. 4a) that have been linked to the pathogenesis of these respective tumour types[23–26]; however, the exact role of these pathway(s) remains to be determined. Given the growing appreciation of the role that the tumour microenvironment has in regulating the progression of cancer[27,28], it is probable that a combination of multiple factors modulated by Hh pathway inhibition in the stroma would affect the growth characteristics of these tumours. Our results have important implications for the clinical development of Hh pathway antagonists and present a new understanding of the way in which Hh antagonists may slow tumour growth.

METHODS SUMMARY

Cell culture assays. Cells were cultured in triplicate in 0.5% serum-containing medium containing HhAntag (Supplementary Fig. 13), cyclopamine or the anti-SHH monoclonal antibody 5E1 (ref. 29). The concentration of antagonists resulting in 50% inhibition of cell viability at 72 h was determined. Co-culture experiments were carried out by culturing tumour cells with C3H10T1/2 fibroblasts expressing luciferase under a *GLI*-responsive promoter for 24 h. Assessment of endogenous Hh pathway gene expression was performed by culturing cells for 24 h with rSHH and/or Hh antagonists in 0.5% serum-containing medium.

***In vivo* models.** Primary human xenografts were established by direct implantation of surgical material into female CD1 nu/nu mice of 6–8 weeks of age and were serially passaged into larger cohorts of mice for efficacy testing on reaching 200–350 mm^3. HT-29, HT55 and DLD-1 cell lines were established as xenografts by injection into the hind flank of CD1 nu/nu mice with 5×10^6 (HT-29 and HT55) or 10×10^6 (DLD-1) cells. HhAntag, or a close derivative, was resuspended in 0.5% methyl-cellulose, 0.2% Tween-80 (MCT) and administered orally twice daily as indicated. 5E1 or an isotype control (IgG1) were administered at 60 mg kg^{-1} on day 1 followed by 30 mg kg^{-1} weekly by means of intraperitoneal delivery. Tumour volumes were calculated as $(L \times W \times W)/2$, where W represents width and L represents length. Statistical analysis was performed on mean tumour volumes at the end of the study using the Dunnett's test. Conditional (floxed) Smo mice (*Smo*$^{C/C}$) and tamoxifen-inducible *CAGGCre-ER* transgenic mice were obtained from A. McMahon.

Gene expression profiling. Microarray gene expression analysis was carried out on Affymetrix Human Genome U133 Plus 2.0 (Supplementary Information File 1) or Mouse Genome 430 2.0 arrays (Supplementary Information File 2). Hh pathway genes were quantitatively assessed in frozen human tissue lysates, cell lines or xenograft tissues by Taqman. Assay information can be found in Supplementary Tables 2 and 3.

Full Methods and any associated references are available in the online version of the paper at www.nature.com/nature.

Received 30 April; accepted 14 July 2008.
Published online 27 August 2008.

1. Clement, V., Sanchez, P., de Tribolet, N., Radovanovic, I. & Ruiz i Altaba, A. HEDGEHOG–GLI1 signaling regulates human glioma growth, cancer stem cell self-renewal, and tumorigenicity. *Curr. Biol.* **17**, 165–172 (2007).
2. Stecca, B. *et al.* Melanomas require HEDGEHOG–GLI signaling regulated by interactions between GLI1 and the RAS-MEK/AKT pathways. *Proc. Natl Acad. Sci. USA* **104**, 5895–5900 (2007).
3. Yuan, Z. *et al.* Frequent requirement of hedgehog signaling in non-small cell lung carcinoma. *Oncogene* **26**, 1046–1055 (2007).
4. Thayer, S. P. *et al.* Hedgehog is an early and late mediator of pancreatic cancer tumorigenesis. *Nature* **425**, 851–856 (2003).
5. Karhadkar, S. S. *et al.* Hedgehog signalling in prostate regeneration, neoplasia and metastasis. *Nature* **431**, 707–712 (2004).
6. Berman, D. M. *et al.* Widespread requirement for Hedgehog ligand stimulation in growth of digestive tract tumours. *Nature* **425**, 846–851 (2003).
7. Watkins, D. N. *et al.* Hedgehog signalling within airway epithelial progenitors and in small-cell lung cancer. *Nature* **422**, 313–317 (2003).
8. Ingham, P. W. & McMahon, A. P. Hedgehog signaling in animal development: paradigms and principles. *Genes Dev.* **15**, 3059–3087 (2001).
9. van den Brink, G. R. Hedgehog signaling in development and homeostasis of the gastrointestinal tract. *Physiol. Rev.* **87**, 1343–1375 (2007).
10. Romer, J. T. *et al.* Suppression of the Shh pathway using a small molecule inhibitor eliminates medulloblastoma in *Ptc1*$^{+/-}$*p53*$^{-/-}$ mice. *Cancer Cell* **6**, 229–240 (2004).
11. Frank-Kamenetsky, M. *et al.* Small-molecule modulators of Hedgehog signaling: identification and characterization of Smoothened agonists and antagonists. *J. Biol.* **1**, 10 (2002).
12. Cooper, M. K., Porter, J. A., Young, K. E. & Beachy, P. A. Teratogen-mediated inhibition of target tissue response to Shh signaling. *Science* **280**, 1603–1607 (1998).
13. Kayed, H. *et al.* Indian hedgehog signaling pathway: expression and regulation in pancreatic cancer. *Int. J. Cancer* **110**, 668–676 (2004).
14. Fan, C. M. *et al.* Long-range sclerotome induction by sonic hedgehog: direct role of the amino-terminal cleavage product and modulation by the cyclic AMP signaling pathway. *Cell* **81**, 457–465 (1995).

15. Sasai, K. *et al.* Shh pathway activity is down-regulated in cultured medulloblastoma cells: implications for preclinical studies. *Cancer Res.* **66**, 4215–4222 (2006).
16. Duda, D. G. *et al.* Differential transplantability of tumor-associated stromal cells. *Cancer Res.* **64**, 5920–5924 (2004).
17. Hayashi, S. & McMahon, A. P. Efficient recombination in diverse tissues by a tamoxifen-inducible form of Cre: a tool for temporally regulated gene activation/inactivation in the mouse. *Dev. Biol.* **244**, 305–318 (2002).
18. Long, F., Zhang, X. M., Karp, S., Yang, Y. & McMahon, A. P. Genetic manipulation of hedgehog signaling in the endochondral skeleton reveals a direct role in the regulation of chondrocyte proliferation. *Development* **128**, 5099–5108 (2001).
19. Beachy, P. A., Karhadkar, S. S. & Berman, D. M. Tissue repair and stem cell renewal in carcinogenesis. *Nature* **432**, 324–331 (2004).
20. Fan, L. *et al.* Hedgehog signaling promotes prostate xenograft tumor growth. *Endocrinology* **145**, 3961–3970 (2004).
21. Pola, R. *et al.* The morphogen Sonic hedgehog is an indirect angiogenic agent upregulating two families of angiogenic growth factors. *Nature Med.* **7**, 706–711 (2001).
22. Ingram, W. J., Wicking, C. A., Grimmond, S. M., Forrest, A. R. & Wainwright, B. J. Novel genes regulated by Sonic Hedgehog in pluripotent mesenchymal cells. *Oncogene* **21**, 8196–8205 (2002).
23. Bergmann, U., Funatomi, H., Yokoyama, M., Beger, H. G. & Korc, M. Insulin-like growth factor I overexpression in human pancreatic cancer: evidence for autocrine and paracrine roles. *Cancer Res.* **55**, 2007–2011 (1995).
24. Durai, R., Yang, W., Gupta, S., Seifalian, A. M. & Winslet, M. C. The role of the insulin-like growth factor system in colorectal cancer: review of current knowledge. *Int. J. Colorectal Dis.* **20**, 203–220 (2005).
25. Zeng, G. *et al.* Aberrant Wnt/β-catenin signaling in pancreatic adenocarcinoma. *Neoplasia* **8**, 279–289 (2006).
26. Pasca di Magliano, M. *et al.* Common activation of canonical wnt signaling in pancreatic adenocarcinoma. *PLoS ONE* **2**, e1155 (2007).
27. Bhowmick, N. A., Neilson, E. G. & Moses, H. L. Stromal fibroblasts in cancer initiation and progression. *Nature* **432**, 332–337 (2004).
28. Orimo, A. & Weinberg, R. A. Stromal fibroblasts in cancer: a novel tumor-promoting cell type. *Cell Cycle* **5**, 1597–1601 (2006).
29. Ericson, J., Morton, S., Kawakami, A., Roelink, H. & Jessell, T. M. Two critical periods of Sonic Hedgehog signaling required for the specification of motor neuron identity. *Cell* **87**, 661–673 (1996).

Supplementary Information is linked to the online version of the paper at www.nature.com/nature.

Acknowledgements The authors thank A. McMahon and M. Scott for providing transgenic mice; T. Holcomb, K. Wagner, D. Lee and P. Wen for their assistance in cell line screening; J. Ernst for rSHH, M. Cole for assistance with imaging; S. Louie for assistance with graphics; P. Haverty for assistance with gene expression data; and M. Evangelista, C. Callahan and V. Dixit for comments and discussions. Tissue samples were provided by the Cooperative Human Tissue Network, which is funded by the National Cancer Institute, and the National Center for Research Resources, which is supported by the National Institutes of Health. Other investigators may have received samples from these same tissues.

Author Contributions F.J.d.S. and L.L.R. conceived and directed the project. S.E.G., R.L.Y., S.J.S., T.T., H.T. J.C.M. and K.K. designed and carried out experiments. C.P.A., D.M., L.F., T.J., D.K. and M.N.-P. carried out experiments. R.L.Y., S.E.G. and F.J.d.S. wrote the paper.

Author Information Microarray data are deposited in the NCBI GEO database under accession number GSE11981. The authors declare competing financial interests: details accompany the full-text HTML version of the paper at www.nature.com/nature. Reprints and permissions information is available at www.nature.com/reprints. Correspondence and requests for materials should be addressed to F.J.d.S. (sauvage@gene.com).

METHODS

Reagents, cell lines and cell culture. HhAntag was synthesized as described in Supplementary Fig. 13. Cycopamine was purchased from Toronto Research Chemicals, Inc. The mouse anti-Shh monoclonal antibody 5E1 (ref. 29) was protein-A-purified and confirmed for lack of aggregation and endotoxin, as well as the ability to block ligand-activated Hh signalling, after gel filtration.

HEPM cells[30] were stably transfected with a luciferase reporter gene driven by six continuous repeats of the *GLI* DNA-binding element. The human colon fibroblast line CCD-18Co was purchased from ATCC (CRL-1459). MEFs from *CAGGCre-ER;Smo*$^{C/C}$ and control mice were isolated according to published methods and treated with tamoxifen (1 μM) *in vitro* for 5 days before testing for Hh responsiveness *in vitro* and/or mixing with HT29-*luc* cells for implantation into CD1 nude mice.

Cell viability was measured at 72 h using the Celltiter-Glo Luminescent Cell Viability Assay kit (Promega), and the concentration of HhAntag resulting in 50% inhibition of cell viability was determined from a minimum of two experiments. Co-culture experiments were carried out by culturing tumour cells at a 4:1 ratio with C3H10T1/2 S12 fibroblast *GLI*-reporter cells[11]. Luciferase activity was measured using the SteadyLite HTS kit (Promega) after 24 h. Assessment of Hh pathway target gene expression was performed by culturing cells in triplicate in 24-well plates for 24 h with 300 ng ml^{-1} rSHH and/or Hh antagonists in 0.5% serum-containing medium. RNA was isolated using Qiagen RNeasy Mini Kit.

Reporter gene assays. Twenty-four hours after plating, cells were transfected for 18 h with either *GLI*-luciferase or *NFκB*-luciferase reporter plasmids in combination with a control herpes simplex virus thymidine kinase (*HSV-TK*)-luciferase plasmid using the Fugene6 transfection reagent (Roche) and then re-plated into 96-well culture plates. Six hours later, Hh antagonist and/or 1 μg ml^{-1} rSHH were added to cells in quadruplicate in 0.5% serum-containing medium. Cultures were re-fed 24 h later, and plates were assessed for firefly and *Renilla* luciferase activity after an additional 24 h using the Promega Dual-Glo luciferase kit.

Immunofluorescence. To evaluate Hh pathway activation *in vivo*, *Ptch1-lacZ;Rag2*$^{-/-}$ mice were implanted with pancreatic tumour cells lines expressing differential levels of Hh ligands. Fourteen days after implantation, xenografts were excised and fixed in 4% paraformaldehyde before embedding in OCT (frozen tissue matrix). Sections were incubated with anti-β-galactosidase (1:10,000, Cappel) and FITC-conjugated anti-ESA (epithelial specific antigen, 1:100, Biomeda) overnight (16 h), followed by secondary Cy3-anti-rabbit (1:400, Jackson Immunoresearch) incubation for one hour. Nuclei were visualized with 4,6-diamidino-2-phenylindole (DAPI, blue) in Vectamount (Vector Laboratory).

Xenograft models. Primary tumour samples were provided by the National Disease Research Interchange (NDRI) and the Cooperative Human Tissue Network, which is funded by the National Cancer Institute. Other investigators may have received samples from these same tissues. Primary human xenografts were established by direct implantation of surgical material into female CD1 nu/nu mice of 6–8 weeks of age (Charles River Laboratories, Inc.). All mice were housed and maintained according to the animal use guidelines of Genentech, Inc., conforming to California State legal and ethical practices. Tissue specimens were shipped in RPMI-containing antibiotics on wet ice and implanted within 24 h after rinsing in DMEM containing 0.11 mg ml^{-1} sodium pyruvate, 1.125 μg ml^{-1} amphotericin B and 1 mg ml^{-1} kanamycin. Tissue was minced with scalpels to a size of $<1\,mm^3$, and approximately 100 mg of tissue was implanted in the subcutaneous space of the hind flank using blunt dissection and a 10G trocar. Tumour lines were serially passaged into larger cohorts of mice for efficacy testing. Mice were distributed into tumour-volume-matched cohorts when tumours reached between 200 mm^3 and 350 mm^3. HT-29, HT55 and DLD-1 cell lines were purchased from ATCC and were established as xenografts by injection into the hind flank of 6–8-week-old female CD1 nu/nu mice with 5×10^6 (HT-29 and HT55) or 10×10^6 (DLD-1) cells resuspended in Hanks' balanced salt solution. Tumour-bearing mice were distributed into tumour-volume-matched cohorts when the tumours reached between 80 mm^3 and 120 mm^3. HhAntag, or a close derivative, was resuspended in MCT and administered orally twice daily at either 100 or 75 mg kg^{-1} from a 10 mg ml^{-1} suspension as indicated. 5E1 or an isotypic control (IgG1) were dissolved in PBS and administered at 60 mg kg^{-1} on day 1 and then at 30 mg kg^{-1} weekly by intraperitoneal delivery. Tumour volume and animal weights were monitored twice weekly and tumour volume calculated as $(L \times W \times W)/2$.

Expression studies. For the analysis of *SHH* and *IHH* mRNA expression in multiple human tissue specimens, data were obtained from Gene Logic, Inc.

Microarray gene expression analysis of RNA extracted from primary xenograft tissue was carried out on two separate platforms, Human Genome U133 Plus 2.0 and Mouse Genome 430 2.0 arrays (Affymetrix). Preparation of complementary RNA, array hybridizations and subsequent data analysis were carried out using the manufacturers' protocols, with signal intensities being determined by the MAS5.0 algorithm. Hh pathway genes were quantitatively assessed by Taqman and transcript levels were normalized to the housekeeping genes β-glucuronidase (*GUSB*) or ribosomal protein L19 (*RPL19*). Results are expressed as normalized expression values ($=2^{-\Delta Ct}$) or normalized expression relative to a cell line pool representative of multiple tissue types ($=2^{-\Delta\Delta Ct}$), unless otherwise stated. For xenograft model profiling, gene expression in each compartment was normalized to the same species-specific housekeeping gene to ensure that observed differences weren't due to differences in the degree of stromal infiltrate. Correlations in gene expression were evaluated by Spearman rank tests and *P*-values were reported. Sequences of primer/probes are shown in Supplementary Table 3 and species-specificity of human/mouse Taqman assays is confirmed in Supplementary Table 2.

Fluorescence-activated cell sorting. Cells were stained with either mouse anti-Hh antibody 5E1 or isotype control antibody and then followed by biotin-conjugated anti-mouse, streptavidin-phycoerythrin and propidium iodide. Stained live (PI-excluded) cells were analysed on a FacsCalibur, and data were plotted using the FlowJo software package.

30. Yoneda, T. & Pratt, R. M. Mesenchymal cells from the human embryonic palate are highly responsive to epidermal growth factor. *Science* 213, 563–565 (1981).